Turbo Equalization: Adaptive Equalization and Channel Decoding Jointly Optimized

Christophe Laot, Alain Glavieux, and Joël Labat

***Abstract*—This paper deals with a receiver scheme where adaptive equalization and channel decoding are jointly optimized in an iterative process. This receiver scheme is well suited for transmissions over a frequency-selective channel with large delay spread and for high spectral efficiency modulations. A low-complexity soft-input soft-output M-ary channel decoder is proposed. Turbo equalization allows intersymbol interference to be reduced drastically. For most time-invariant discrete channels, the turbo-equalizer performance is close to the coded Gaussian channel performance, even for low signal-to-noise ratios. Finally, results over time-varying frequency-selective channel proves the excellent behavior of the turbo equalizer.**

***Index Terms*—Channel coding, equalizers, fading channel, intersymbol interference.**

I. Introduction

THE DEVELOPMENT of digital communications systems over multipath channels has seen a considerable number of works during the last decade. Indeed, the increasing demand for high spectral efficiency modulation requires regular system evolution in order to improve performance. The increasing data rates through bandlimited channels introduce intersymbol interference (ISI) which drastically deteriorates the received signal. As a consequence, it is necessary for the optimal receiver to deal with this phenomenon in order to achieve acceptable performance.

Conventional solutions generally involve both equalization and channel coding which are done separately. In what follows, we introduce a new receiver scheme, called a turbo equalizer, where adaptive equalization and channel decoding are jointly optimized in order to improve the global performance. Equalization is achieved by means of an ISI canceller which completely removes ISI when transmitted data are *a priori* known. This assumption is meaningless in practice. Nevertheless, it is possible to obtain a reliable estimate of these data by using information provided by a previous processing involving both equalization and channel decoding. A turbo equalizer [1]–[3] allows the receiver to benefit from channel decoder gain thanks to an iterative process applied to the same data block.

In fact, the turbo-equalizer performance depends on channel selectivity and/or its time variation. For a large number of time-invariant channels, the turbo equalizer succeeds in completely removing the ISI and exhibits the same performance as the coded additive white Gaussian noise channels (AWGN). For time-varying channels, the turbo equalizer eliminates ISI and leads to a diversity gain.

Although the turbo equalizer is an original approach to combat ISI, many authors have already proposed solutions using an ISI canceller, a maximum likelihood sequence estimator (MLSE), and a channel decoder.

In 1981, Gersho and Lim [4] and Mueller and Salz [5] proposed an equalizer including a matched filter followed by a linear ISI canceller which uses past and/or future transmitted data. When data are known, this equalizer totally overcomes ISI. In other cases, a linear equalizer estimates data previously. Due to this, the receiver performance is strongly dependent on the bit error rate (BER) at the linear equalizer output. Furthermore, this receiver cannot benefit from information provided by a channel decoder.

Many years later, Eyuboglu [6] proposed a receiver combining a decision feedback equalizer (DFE), a channel decoder, and a periodic interleaver. With this approach, the equalizer can use hard decisions provided by the channel decoder. For a low BER at the decoder output, this receiver can reach optimum DFE and coding performance. This receiver is thus very sensitive to decoding errors. Later, Zhou and Proakis [7] added an iterative process to this system in order to improve adaptive parameter estimation. The performance of such a receiver is largely suboptimum when the channel is strongly frequency-selective.

Finally in 1995, a receiver called a turbo-detector [8], [9], whose principle is borrowed from turbo-codes [10], combined a maximum *a posteriori* (MAP) detector with a MAP decoder through an iterative process. The performance has proved to be near optimum for many transmission channels. Nevertheless, the turbo-detector is essentially dedicated to weak spectral efficiency modulations and a channel exhibiting a weak delay spread owing to prohibitive computational complexity. In order to reduce the turbo-detector complexity, the MAP detector can be advantageously replaced by an ISI canceller. This new receiver, called a turbo-equalizer [1]–[3], makes it possible to almost completely overcome ISI over time-invariant and/or time-varying Rayleigh channels for high spectral efficiency modulations.

This paper presents the turbo-equalizer scheme and its performance. It is organized as follows. Section II describes the transmission model where the information data are coded, interleaved, and then transmitted over a frequency-selective channel, using M-QAM signaling. Section III introduces the turbo-equalizer structure which combines an adaptive equalizer called an interference canceller, a deinterleaver, a soft-input

Manuscript received May 1, 2000; revised December 1, 2000, and March 1, 2001. This work was supported in part by FTR&D, DMR/DDH.

The authors are with ENST Bretagne, BP 832, 29285 Brest Cedex, France (e-mail: christophe.laot@enst-bretagne.fr; alain.glavieux@enst-bretagne.fr; joel.labat@enst-bretagne.fr).

Publisher Item Identifier S 0733-8716(01)04188-9.

0733–8716/01$10.00 © 2001 IEEE

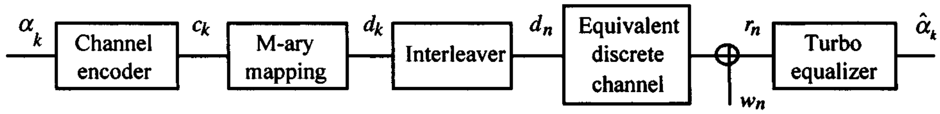

Fig. 1. Principle of the transmission scheme.

soft-output decoder for M-ary symbols, and an interleaver, the whole process being iteratively repeated. Section IV provides simulation results for 4-QAM, 16-QAM, and 64-QAM over frequency-selective channels. Section V presents our conclusions.

II. Principle of the Transmission Scheme

Let us consider the transmission scheme depicted in Fig. 1. A rate R convolutional code is fed in by independent binary data α_k taking the values 0 or 1 with the same probability. Each set of 2-m encoded data $c_{k,i}$; $i = 1, \ldots, 2m$ is associated with M-ary complex symbol $d_k = (a_k + jb_k)/\sigma$ where symbols a_k and b_k with variance $\sigma^2/2$ take equiprobable values in the set $\{\pm 1, \pm 3, \ldots, \pm(\sqrt{M-1})\}$ with $\sqrt{M} = 2^m$. Symbols d_k with symbol duration T and unitary variance σ_d^2 are then interleaved and called d_n.

The signal at the output of the equivalent discrete channel is corrupted by an AWGN w_n with variance σ_w^2. The observed channel noisy output r_n can be written

$$r_n = \sum_{l=0}^{L} h_l d_{n-l} + w_n \tag{1}$$

where h_l are the coefficients of the discrete channel impulse response, which produces ISI. In this approach, the channel is considered time-invariant.

The transfer function of this channel is given by

$$H(f) = \sum_{l=0}^{L} h_l \exp(-j2\pi f l T). \tag{2}$$

The signal-to-noise ratio (SNR) at the turbo-equalizer input is equal to

$$\text{SNR} = \frac{\sigma_d^2 hh_0}{\sigma_w^2} = R\,\frac{E_b}{N_0}\,\log_2(M) \tag{3}$$

where

- E_b the mean energy received by information data;
- N_0 the monolateral noise power spectral density at the input of the receiver;
- hh_l the autocorrelation channel function defined by

$$hh_l = \sum_{i=-\infty}^{\infty} h_i h_{i-l}^*. \tag{4}$$

III. Turbo-Equalizer Structure

For a turbo equalizer, equalization and channel decoding are jointly performed in an iterative way as for a turbo-decoder [10]. Each iteration p; $p = 1, \ldots, P$ is carried out by a module fed in by both samples $r_n^{(p-1)}$ and decoded data $\overline{d}_n^{(p-1)}$ originating from the module $(p-1)$. The turbo-equalizer scheme is depicted in Fig. 2 where the delays are equal to the latency of each module.

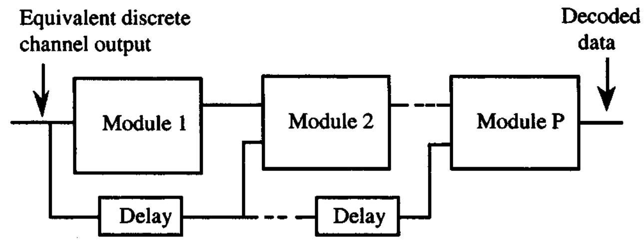

Fig. 2. Turbo-equalizer principle.

Each module consists of an equalizer, a deinterleaver, a symbol-to-binary converter (SBC), a soft-input soft-output (SISO) binary decoder, a binary to symbol converter (BSC), and an interleaver as depicted in Fig. 3. Each module p provides an estimation of the symbol d_n, called $\overline{d}_n^{(p)}$. This information will be used by the adaptive equalizer of the next module. Note that a module uses the same SISO binary decoder for all M-ary modulations. In this principle scheme, the combination of the three functions SBC, SISO binary decoder, and BSC constitutes an approximation of a SISO M-ary decoder.

A. Equalizer Structure

The equalizer is close to an intersymbol interference canceller (IC) which allows ISI to be completely removed, providing that symbols d_n are known. Generally these symbols are unknown by the receiver. As a consequence, the equalizer is a suboptimum IC which replaces transmitted symbols by $\overline{d}_n^{(p)}$ symbols estimated by the previous module p and adjusts its filters coefficients in an adaptive way. When the SNR is sufficient, the iterative process gradually increases the reliability of the estimated symbols and the adaptive equalizer reaches the performance of the optimum IC. Fig. 4 depicts the equalizer structure, consisting of two transversal filters fed by the received samples $r_n^{(p)}$ and the data $\overline{d}_n^{(p)}$, respectively, estimated from the previous module.

For each stage, the equalizer is updated according to the mean-square-error (MSE) criterion defined as

$$\text{MSE} = E\{|s_n - d_n|^2\} \tag{5}$$

where the superscript p has been dropped for convenience.

In order to determine the optimum IC, it is necessary to assume that the symbols $(\overline{d}_n = d_n)$ are known. With the constraint for the central coefficient of the filter $Q(f)$ having to be equal to zero $(q_0 = 0)$, it can be shown [4], [5] that the IC optimum filters have the following transfer function:

$$P(f)_{\text{opt}} = \beta\,\frac{H^*(f)}{hh_0} = \sum_{l=0}^{L} p_l \exp(-j2\pi f l T) \tag{6}$$

$$Q(f)_{\text{opt}} = \beta\left(\frac{|H(f)|^2}{hh_0} - 1\right) = \sum_{l=-L}^{L} q_l \exp(-j2\pi f l T) \tag{7}$$

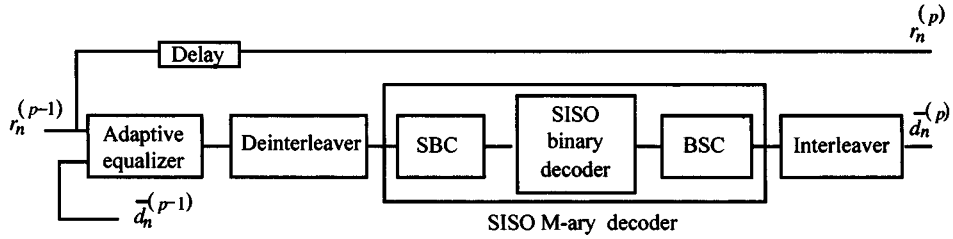

Fig. 3. Principle scheme of module $p-1$.

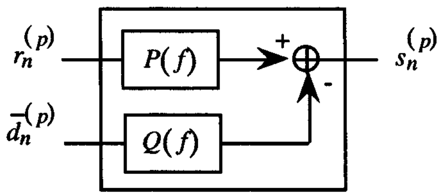

Fig. 4. Equalizer structure.

where the weighting coefficient β is equal to

$$\beta = \sigma_d^2 h h_0 / (\sigma_d^2 h h_0 + \sigma_w^2) \tag{8}$$

and p_l and q_l are the coefficients of filters $P(f)$ and $Q(f)$, respectively.

Thus, the IC output is ISI-free and equal to

$$s_n = \beta \left(d_n + \frac{1}{hh_0} \sum_{l=0}^{L} h_l^* w_{n+l} \right) \tag{9}$$

with the output MSE given by

$$\text{MSE}_{\text{opt}} = \sigma_d^2 \sigma_w^2 / (\sigma_d^2 h h_0 + \sigma_w^2) = 1 - \beta \tag{10}$$

and the SNR at the IC output is equal to

$$\text{SNR}_{\text{opt}} = \sigma_d^2 h h_0 / \sigma_w^2. \tag{11}$$

As a consequence of the comparison of (11) with (3), it clearly appears that ISI is completely removed by the equalizer, without noise enhancement.

Transmitted symbols d_n are generally unknown by the receiver and the equalizer is suboptimum because $Q(f)$ is fed in by estimated symbols instead of transmitted symbols. This suboptimality is taken into account in an adaptive way to adjust the equalizer coefficients. So, at the first iteration $(p = 1)$, the estimated symbols are equal to zero and the equalizer approximates the MMSE linear equalizer. After several iterations $(p > 1)$, the likelihood of the estimated symbols is expected to be right and the adaptive equalizer is close to the optimum IC defined by the transfer function (6) and (7).

B. Adaptive Equalization

Adaptive algorithms [11], [12] such as stochastics gradient least mean square (SGLMS) or recursive least square (RLS) can be used for updating equalizer parameters. These algorithms minimize the MSE defined by (5). In general, they require an initial or even periodic data sequence (learning sequence) known by the receiver to ensure the convergence of the algorithms. Once convergence is established, the algorithms are decision-directed and minimize the estimated MSE given by

$$\hat{\text{MSE}} = E\{|s_n - \hat{d}_n|^2\} \tag{12}$$

where $\hat{d}_n = (\hat{a}_n + j\hat{b}_n)/\sigma$ is a tentative decision taken at the equalizer output.

Let u_n and v_n be the normalized phase and quadrature components of the output equalizer, respectively,

$$s_n = \beta(u_n + jv_n) \tag{13}$$

and the decision rules for a M-QAM are

$$\begin{aligned}
\hat{a}_n &= \left(\sqrt{M} - 1\right), && \text{if } \sigma u_n > \left(\sqrt{M} - 2\right) \\
\hat{a}_n &= (2i + 1), && \text{if } 2i < \sigma u_n < (2i + 2) \\
\hat{a}_n &= -(2i + 1), && \text{if } -(2i + 2) < \sigma u_n < -2i \\
\hat{a}_n &= -\left(\sqrt{M} - 1\right), && \text{if } \sigma u_n < -\left(\sqrt{M} - 2\right) \\
& i = 0, \ldots, \sqrt{M}/2 - 1. &&
\end{aligned} \tag{14}$$

Substitution of $\hat{a}_n$ (u_n) by $\hat{b}_n$ (v_n) into the relation (14) gives the $\hat{b}_n$ value.

For each iteration, the equalizer structure is depicted in Fig. 4. Output channel sequence $\mathbf{R_n}$ and estimated symbols sequence $\overline{\mathbf{D}}_\mathbf{n}$ provided by the channel decoder output of the previous module feed the equalizer. The equalizer output is given by

$$s_n = \mathbf{P}_n^t \mathbf{R}_n - \mathbf{Q}_n^t \overline{\mathbf{D}}_n \tag{15}$$

where $\mathbf{R}_n = [r_{n+L_1} \cdots r_n \cdots r_{n-L_1}]^t$ and $\overline{\mathbf{D}}_n = [\overline{d}_{n+L_2} \cdots \overline{d}_n \cdots \overline{d}_{n-L_2}]^t$ are the received samples vector and the estimated mean values vector, respectively. $\mathbf{P}_n = [\hat{p}_{-L_1}(n) \cdots \hat{p}_0(n) \cdots \hat{p}_{L_1}(n)]^t$ and $\mathbf{Q}_n = [\hat{q}_{-L_2}(n) \cdots 0 \cdots \hat{q}_{L_2}(n)]^t$ are the equalizer parameters vector corresponding to filters $P(f)$ and $Q(f)$, respectively. L_1 and L_2 are appropriate values greater or equal to L. t denotes the transposition.

For a time-invariant channel, the SGLMS algorithm is used for all iterations $(p \geq 1)$ and initialized by a learning sequence at the beginning of the transmission. Corresponding update equations are given by

$$\mathbf{P}_{n+1} = \mathbf{P}_n - \mu \mathbf{R}_n^* (s_n - \hat{d}_n) \tag{16}$$

$$\mathbf{Q}_{n+1} = \mathbf{Q}_n + \mu \overline{\mathbf{D}}_n^* (s_n - \hat{d}_n) \tag{17}$$

where μ is an appropriate step size.

For a time-varying channel, the RLS algorithm is used for all iterations $(p \geq 1)$ and data aided by a periodic learning sequence. At the first iteration $(p=1)$, the estimated symbols $\overline{d}_n$ are unknown and the equalizer is a purely adaptive transversal filter. For the other iterations $(p>1)$ and from relations (6) and (7), the equalizer coefficients p_l and q_l can be calculated with

$$p_l = \beta h^*_{L-l}/hh_0 \tag{18}$$

$$q_l = \beta hh_l/hh_0 \qquad l \neq 0 \quad \text{and} \quad q_0 = 0. \tag{19}$$

Generally, channel coefficients are unknown and can be estimated by an RLS algorithm.

The substitution of h_l with its estimated value $\hat{h}_l(n)$ in (18) and (19) allows the equalizer coefficient to be approximated. The advantage of this approach is to have a smaller number of taps to be adjusted in order to enable the algorithm to follow channel fluctuation rapidly. However, this approach does not take into account the suboptimality of IC during the very first iterations.

Some modifications can improve the performance of the adaptive equalizer. To increase the speed of the convergence, $\hat{d}_n$ and $\overline{d}_n$ can be substituted with d_n in (12), (15), (16), and (17) during the learning sequence. For the iteration $(p>1)$, decisions on estimated symbols $\overline{d}_n$ are more accurate than tentative decisions at the equalizer output and replace $\hat{d}_n$ in (12), (16), and (17). Furthermore, when a frequency offset exists between the transmitter and receiver oscillators, the equalizer can integrate a phase-locked loop (PLL) [13].

C. Interleaving and Deinterleaving Functions

The interleaving function allows temporal error sequence distribution to be modified and splits the error series. Used generally with time-varying channels, the interleaver is an essential function of the turbo-equalizer even if the channel is time-invariant. Over a severe frequency-selective channel, the likelihood of the estimated data is weak and the equalizer output presents series of errors with large values which perturbates the channel decoder. Due to this, the interleaving dimension may be sufficient in comparison with the error sequence length but also in comparison with the error value. Some results related to interleaving performance versus interleaver size are given in Section IV.

As presented in Fig. 1, the turbo-equalizer interleaves symbols d_n. An alternative approach is to replace the symbol-interleaver by a bit-interleaver located between the channel encoder and the mapper. This approach is often used and gives excellent performance. Nevertheless, it can be demonstrated [1] that theoretical bounds for high-order modulation give better performance with a symbol-interleaver than a bit-interleaver.

It is for this reason that our turbo-equalizer uses a matrix $N \times N$ interleaver on symbols. Symbols d_n are written line by line in a matrix and read following a given rule.

For the uniform rule, the relations between a coordinate input couple (i_n, j_n) associated with the symbol d_n and the output coordinates (i_k, j_k) associated with the symbol d_k are given by $(i_k, j_k) = (j_n, i_n)$.

For the nonuniform rule, the relations between the input couple (i_n, j_n) and the output couple (i_k, j_k) are given by

$$\begin{aligned} i_k &= 2 \operatorname*{mod}_{N/2}(x) + 1 && \text{if } i_n \text{ is even} \\ i_k &= 2 \operatorname*{mod}_{N/2}(x) && \text{if } i_n \text{ is odd} \\ j_k &= 2 \operatorname*{mod}_{N}(j_n y) \end{aligned}$$

where mod_N means modulo N.

Parameters x and y are, respectively, equal to

$$\begin{aligned} x &= \frac{2j_n + i_n}{2}, && \text{if } i_n \text{ is even} \\ x &= \frac{2j_n + i_n - 1}{2}, && \text{if } i_n \text{ is odd} \end{aligned}$$

and

$$\begin{aligned} &y = 7, && \text{if } z = 0 && y = 29, && \text{if } z = 4 \\ &y = 17, && \text{if } z = 1 && y = 13, && \text{if } z = 5 \\ &y = 11, && \text{if } z = 2 && y = 21, && \text{if } z = 6 \\ &y = 23 && \text{if } z = 3 && y = 19, && \text{if } z = 7 \end{aligned}$$

where z is equal to $x \mod 8$.

Nonuniform interleaving in comparison with uniform interleaving allows the matrix size to be reduced for equivalent performance.

D. Symbol to Binary Converter (SBC)

This function enables the same channel decoder to be used regardless of the state number of the M-QAM modulation. The SBC associates values $\Lambda(c_{k,i})$, representative of $2m$ binary coded data $c_{k,i}$; $i = 1, 2, \ldots, 2m$, at each sample $s_k = \beta(u_k + jv_k)$ provided by the equalizer $2m$. Values $\Lambda(c_{k,i})$ are defined as the logarithm of the likelihood ratio (LLR) of binary coded data conditionally to the observation u_k (v_k) representative of symbol a_k (b_k)

$$\begin{aligned} \Lambda(c_{k,i}) &= K \ln \frac{\Pr\{c_{k,i} = 1/u_k\}}{\Pr\{c_{k,i} = 0/u_k\}}, && i = 1, \ldots, m \\ \Lambda(c_{k,i}) &= K \ln \frac{\Pr\{c_{k,i} = 1/v_k\}}{\Pr\{c_{k,i} = 0/v_k\}}, && i = m+1, \ldots, 2m \end{aligned} \tag{20}$$

where K is a constant. Its value will be defined later.

A symbol a_k is a representative form of a binary coded data vector, with dimension m, such that $\mathbf{c_k} \equiv (c_{k,1}, \ldots, c_{k,i}, \ldots, c_{k,m})$. Let us denote $a_k(\mathbf{c_k})$ the symbol a_k associated with one among 2^m possible realizations of $\mathbf{c_k}$. By fixing $c_{k,i} = j$; $j = 0, 1$, we define a new vector $\mathbf{c_k}$: $c_{k,i} = j$ that has 2^{m-1} possible realizations. By applying Bayes' rule, the LLR given by (20) may be written as

$$\Lambda(c_{k,i}) = K \ln \frac{\displaystyle\sum_{\mathbf{c_k}:\, c_{k,i}=1} p\{u_k/\mathbf{c_k}\}}{\displaystyle\sum_{\mathbf{c_k}:\, c_{k,i}=0} p\{u_k/\mathbf{c_k}\}} \qquad i = 1, \ldots, m \tag{21}$$

where $p\{u_k/\mathbf{c_k}\}$ is the probability density function (pdf) of observation u_k conditionally to the transmitted symbol $\mathbf{c_k}$. This pdf follows a Gaussian law according to (9) and (13) and the LLR may be expressed as

$$\Lambda(c_{k,i}) = K \ln \frac{\displaystyle\sum_{\mathbf{c_k}:\, c_{k,i}=1} \exp\left(-\frac{hh_0}{\sigma^2\sigma_w^2}(\sigma u_k - a_k(\mathbf{c_k}))^2\right)}{\displaystyle\sum_{\mathbf{c_k}:\, c_{k,i}=0} \exp\left(-\frac{hh_0}{\sigma^2\sigma_w^2}(\sigma u_k - a_k(\mathbf{c_k}))^2\right)} \qquad i = 1, \ldots, m. \tag{22}$$

The complexity of the previous relation can be reduced by using the Logarithm Jacobian defined by

$$\ln(\exp(-x) + \exp(-y)) = -\min(x, y) + \ln(1 + \exp(-|x - y|)). \tag{23}$$

When the distance between x and y is sufficiently large, it is possible to write

$$\ln(\exp(-x) + \exp(-y)) \approx -\min(x, y). \tag{24}$$

In this case, for a sufficiently large SNR, the LLR may be approximated by

$$\Lambda(c_{k,i}) \approx K \frac{hh_0}{\sigma^2\sigma_w^2}\left[\min_{\mathbf{c_k}:\, c_{k,i}=0}(\sigma u_k - a_k(\mathbf{c_k}))^2 - \min_{\mathbf{c_k}:\, c_{k,i}=1}(\sigma u_k - a_k(\mathbf{c_k}))^2\right]. \tag{25}$$

For $K = \sigma^2\sigma_w^2/4hh_0$, the estimation of coded data provided to the SBC is only a function of the equalizer output and is given by

$$\Lambda(c_{k,i}) = \frac{1}{4}\left[\min_{\mathbf{c_k}:\, c_{k,i}=0}(\sigma u_k - a_k(\mathbf{c_k}))^2 - \min_{\mathbf{c_k}:\, c_{k,i}=1}(\sigma u_k - a_k(\mathbf{c_k}))^2\right]. \tag{26}$$

Fixing K to the previous value simplifies the receiver complexity because the noise variance disappears and its estimation is not necessary.

Consideration of a particular mapping for a coded bit can simplify this expression. The mapping associates an m-bit vector with a symbol. When two adjacent m-bit symbols differ by only a single bit, as depicted in Fig. 5, the encoding (Gray mapping) allows the BER to be minimized.

With Gray mapping, (26) can be approximated by

$$\begin{aligned}\Lambda(c_{k,m}) &= (\sigma|u_k| - 2^{m-1})\\ \Lambda(c_{k,i}) &= (|\Lambda(c_{k,i+1})| - 2^{i-1}) \qquad i = (m-1), \ldots, 2\\ \Lambda(c_{k,1}) &= \sigma u_k\end{aligned} \tag{27}$$

and in the same manner

$$\begin{aligned}\Lambda(c_{k,2m}) &= (\sigma|v_k| - 2^{m-1})\\ \Lambda(c_{k,m+i}) &= (|\Lambda(c_{k,i+1+m})| - 2^{i-1})\\ &\qquad i = (m-1), \ldots, 2\\ \Lambda(c_{k,m+1}) &= \sigma v_k.\end{aligned} \tag{28}$$

The difference between the exact LLR (22) and its approximation (27) has been evaluated and the loss is weak with respect to the calculation gain [14].

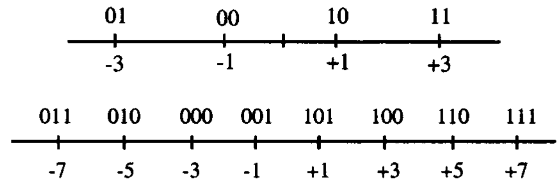

Fig. 5. Example of Gray mapping for 16-QAM and 64-QAM modulations.

E. Soft-Input Soft-Output (SISO) Channel Decoder

The channel decoder is a SISO which is an approximate version of the MAP algorithm [15]. These outputs are given by the LLR of coded data

$$\tilde{\Lambda}(c_{k,i}) = \ln \frac{\Pr\{c_{k,i} = 1/obs\}}{\Pr\{c_{k,i} = 0/obs\}} \tag{29}$$

where the observations, called obs, are the samples $\Lambda(c_{k,i})$ provided by the SBC.

Equation (29) has been determined from the Berrou–Adde algorithm [16]. This algorithm is less optimum than other algorithms but gives good performance with reasonable complexity requirements [15].

F. Binary-to-Symbol Converter (BSC)

To feed the equalizer filter $Q(f)$ it is necessary for the transmitted symbols to be known or estimated. When transmitted symbols are unknown, it is possible to get an estimated value $\overline{d}_n = \overline{a}_n + j\overline{b}_n$ from coded data LLRs provided by the channel decoder of the previous module. This paragraph proposes a solution to convert the binary decoder output to an M-ary symbol.

As previously, $a_n(\mathbf{c_n})$ denotes the symbol a_n associated with one among 2^m possible realizations of $\mathbf{c_n}$. Then, estimated $\overline{a}_n$ of a_n may be approximated by its mean value

$$\begin{aligned}\overline{a}_n &= E\{a_n(\mathbf{c_n})/\mathbf{c_n},\, obs\}\\ &= \sum_{\mathbf{c_n}} a_n(\mathbf{c_n}) \Pr\{a_n = a_n(\mathbf{c_n})/\mathbf{c_n},\, obs\}.\end{aligned} \tag{30}$$

By using the fact that coded data are decorrelated, this expression may be written as

$$\overline{a}_n = \sum_{\mathbf{c_n}} a_n(\mathbf{c_n}) \prod_{i=1}^{m} \Pr\{c_{n,i} = c_{n,i}(\mathbf{c_n})/\mathbf{c_n},\, obs\}. \tag{31}$$

Let us consider the case of a 4-QAM modulation. Symbol $a_n(\mathbf{c_n})$ is associated with one coded piece of data $\mathbf{c_n} = (c_{n,1})$ and has two possible values. The estimated symbol is equal to

$$\overline{a}_n = (1)\Pr\{c_{n,1} = 1/obs\} + (-1)\Pr\{c_{n,1} = 0/obs\}. \tag{32}$$

From (29), when coded data are independent and identically distributed (i.i.d), the LLR of coded data is equal to

$$\tilde{\Lambda}(c_{n,i}) = \ln \frac{\Pr\{c_{n,i} = 1/obs\}}{1 - \Pr\{c_{n,i} = 0/obs\}} \tag{33}$$

the probability of having $c_{n,i} = 1$ may be expressed by

$$\Pr\{c_{n,i} = 1/obs\} = \frac{\exp\left(\tilde{\Lambda}(c_{n,i})\right)}{1 + \exp\left(\tilde{\Lambda}(c_{n,i})\right)}. \tag{34}$$

Consequently, by substituting (34) into (32), the estimated symbol is

$$\overline{a}_n = \frac{\exp\left(\tilde{\Lambda}(c_{n,1})\right) - 1}{\exp\left(\tilde{\Lambda}(c_{n,1})\right) + 1} = \tanh\left(\frac{\tilde{\Lambda}(c_{n,1})}{2}\right). \quad (35)$$

$\overline{b}_n$ may be obtained in the same way. For high-order modulation, (32) must be changed according to the Gray mapping described in Fig. 5.

IV. Simulation Results

A. Time-Invariant Channels

For simulations, the information data were coded by a 1/2 rate convolutional code with a free distance equal to 7 and generator polynomials equal to 23, 35 (expressed in octals). Turbo-equalizer performance was evaluated for M-QAM signaling schemes ($M = 4$, 16, and 64) with several discrete equivalent channel responses. Time-invariant channels may be characterized by their coefficients vector $\mathbf{H} = [h_0;\ \ldots;\ h_L]^t$. Simulations use equivalent discrete channels proposed by Porat and Friedlander [17] and Proakis [11]:

$$\begin{aligned}\mathbf{H}_{\text{Porat \& al}} &= [2 - 0.4j;\ 1.5 + 1.8j;\ 1;\\ &\quad\ 1.2 - 1.3j;\ 0.8 + 1.6j]^t\\ \mathbf{H}_{\text{Proakis A}} &= [0.04;\ -0.05;\ 0.07;\ -0.21;\ -0.5;\ 0.72;\\ &\quad\ 0.36;\ 0;\ 0.21;\ 0.03;\ 0.07]^t\\ \mathbf{H}_{\text{Proakis B}} &= [0.407;\ 0.815;\ 0.407]^t.\end{aligned}$$

The output channel power was normalized to unity. Considering data with variance $\sigma_d^2 = 1$, it is necessary to normalize the coefficients vector by fixing $hh_0 = 1$. For each simulation, we have represented by a dashed line the theoretical bound of the turbo-equalizer, which corresponds to an IC fed by transmitted symbols. At the IC output, ISI is completely cancelled and transmitted symbols are only corrupted by a correlated noise. This noise is whitened by interleaving, allowing the channel decoder to run under optimal conditions. For a multipath time-invariant channel, the theoretical bound of the turbo-equalizer corresponds to the performance of Gaussian channel with coding. The turbo-equalization goal is to reach this limit.

From theoretical results, the turbo-equalizer needs parameter β in order to run. This parameter is given by (10) and can be estimated by $\hat{\beta}_n = 1 - E\hat{Q}M_n$ with $E\hat{Q}M_n = \lambda E\hat{Q}M_{n-1} + (1-\lambda)|s_n - \hat{d}_n|$, where $\hat{d}_n$ corresponds to the decision symbol from equalizer output at the first iteration and at the decision symbol from BSC output for the other iterations, respectively. λ is a positive constant denoting the forgetting factor equal to 0.995.

To allow equalizer convergence a training sequence made up of 2048 symbols is transmitted. At the first iteration, the number of tap weights of $P(f)$ is equal to 31, the central coefficient of the filter is initialized to 1 and adaptation step sizes for SGLMS algorithms are equal to 0.003 for the training period and 0.0005 for the tracking period. For the other iterations, the number of taps is equal to 21 for $P(f)$ and 41 for $Q(f)$, respectively, and the central tap of $P(f)$ filter is initialized to 1. The adaptation step size for SGLMS algorithms is equal to 0.003 for the training period and 0.000 25 for the tracking period.

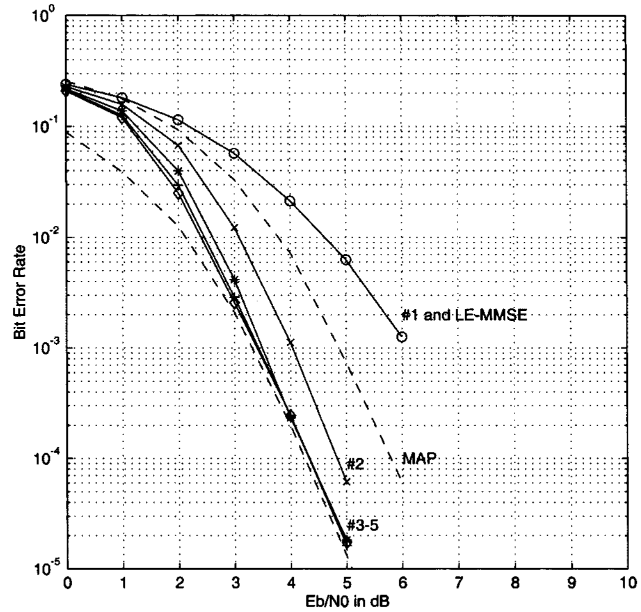

Fig. 6. Turbo-equalization performance over the Porat and Friedlander channel for a 4-QAM modulation.

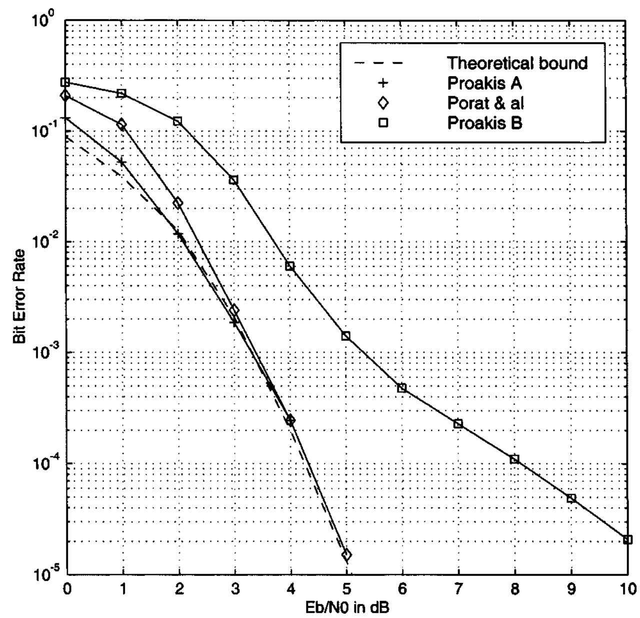

Fig. 7. Turbo-equalization performance over several channels for a 4-QAM modulation at the fifth iteration.

The BER versus E_b/N_0 was evaluated in the tracking period over coded data using the Monte Carlo method (for at least 100 transmission errors. For results presented in Figs. 6–9, a 64 × 64 matrix following a uniform law as defined in Section III-C performed the interleaving.

Fig. 6 depicts the BER at the output of the turbo-equalizer as a function of the number of iterations p, for a 4-QAM modulation over the Porat and Friedlander channel. For this channel, only three iterations and an SNR greater than 3 dB are necessary for the performance of a coded Gaussian channel without ISI to be reached. Thus, for a sufficiently large SNR, the turbo-equalizer

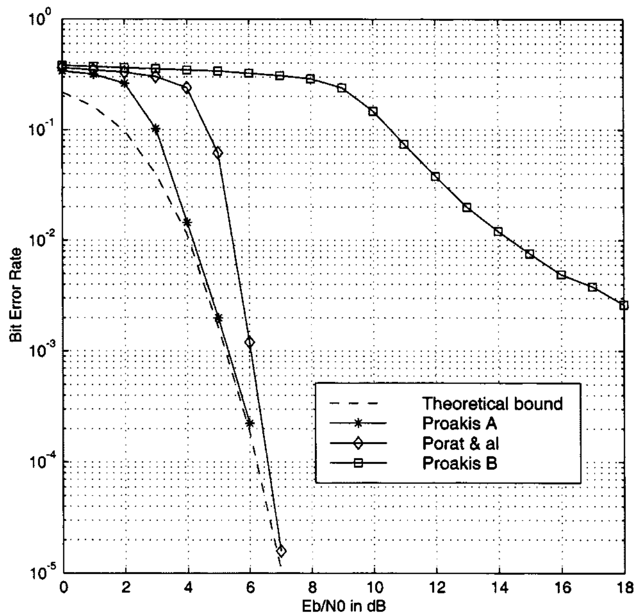

Fig. 8. Turbo-equalization performance over several channels for a 16-QAM modulation at the fifth iteration.

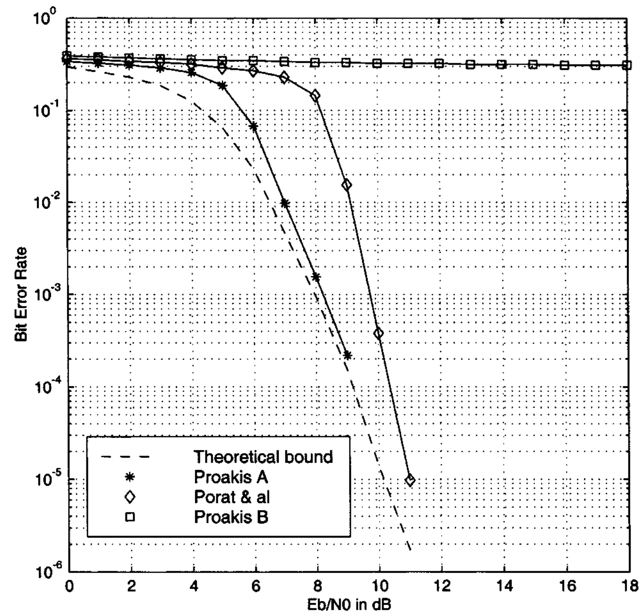

Fig. 9. Turbo-equalization performance over several channels for a 64-QAM modulation at the fifth iteration.

improves its global performance at each iteration and reaches the theoretical bound, provided that a sufficient number of iterations is processed. In fact, the "turbo effect" is primed when the estimated data feeding the equalizer reach a BER threshold sufficiently low allowing the equalizer to cancel a large amount of ISI. This BER threshold depends on the first iteration performance which is mainly a function of the transversal equalizer performance and channel coding gain.

The performance comparison with linear MMSE equalizer (LE-MMSE) and MAP detector is shown in Fig. 6. The performance of the LE-MMSE equalizer corresponds to the first iteration $(p = 1)$ of the turbo-equalizer. It worth noting that for a low SNR the adaptive Decision Feedback Equalizer (DFE-MMSE) presents approximately the same performance as the LE-MMSE. Table I presents some performance comparisons between different receivers for a BER equal to 10^{-3}.

Fig. 7 presents the turbo-equalizer performance for a 4-QAM modulation over the three previously mentioned channels, at the fifth iteration. The turbo-equalizer over Proakis A and Porat *et al.* channels totally overcomes the ISI, even for weak SNRs. However, for the Proakis B channel, the turbo-equalizer does not enable the theoretical bound to be reached. For this channel, an error introduced at the $Q(f)$ input filter creates an impulse noise at the output of the equalizer that strongly affects the channel decoder and decreases the channel coding gain. This phenomenon appears for highly frequency-selective channels. To improve the turbo-equalizer performance over these channels one can increase the interleaver size as described below.

Fig. 8 presents the turbo-equalizer performance for a 16-QAM modulation over the three previous channels at the fifth iteration. Like in Fig. 7, the performance of the turbo-equalizer over Proakis A and Porat *et al.* channels roughly reaches the theoretical bound, whereas, for the Proakis B channel performance is poor. From a general point of view, using large spectral efficiency modulation increases the pathological behavior over severe frequency selective channels. Note that, in terms of complexity, a MAP detector over the Porat *et al.* channel for MAQ16 needs a trellis with 65 536 states whereas the turbo-equalizer uses simple filters for better performance.

TABLE I
PERFORMANCE COMPARISON BETWEEN DIFFERENT RECEIVERS OVER THE PORAT AND FRIEDLANDER CHANNEL FOR A 4-QAM MODULATION

BER equal to 10-3	Eb/N0 in dB	Complexity
Gaussien coded channel	3.3	Theoretical bound
Turbo-equalizer	3.35	Linear filters
MAP	4.8	Treillis 256 states
LE-MMSE	6.2	Linear filters
DFE-MMSE	6.2	Linear filters

The performance achieved at the fifth iteration for a 64-QAM modulation over the three previously described channels is represented in Fig. 9. The turbo-equalizer reaches the theoretical bound when the SNR is greater than 8 dB for the Proakis A channel and 11 dB for the Porat *et al.* channel, respectively. The poor performance of the transversal equalizer at the first iteration over the Proakis B channel for a 64-QAM does not allow the turbo-effect to be started and the performance is worse.

Fig. 10 presents the turbo-equalizer performance at the fifth iteration as a function of the interleaver type and size over the Proakis B channel for a 4-QAM modulation. When the interleaver size is sufficient, the turbo-equalizer performance reaches the theoretical bound. If the interleaver size decreases

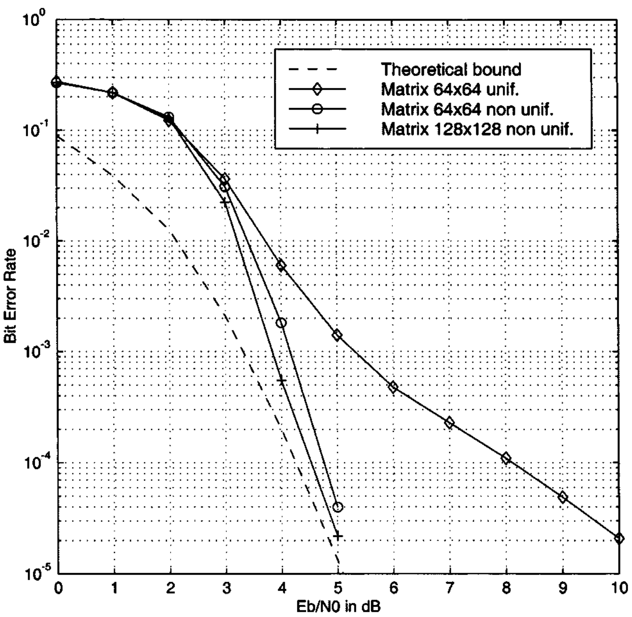

Fig. 10. Turbo-equalization performance over the Proakis B channel for a 4-QAM modulation at the fifth iteration as a function of the interleaver type and size.

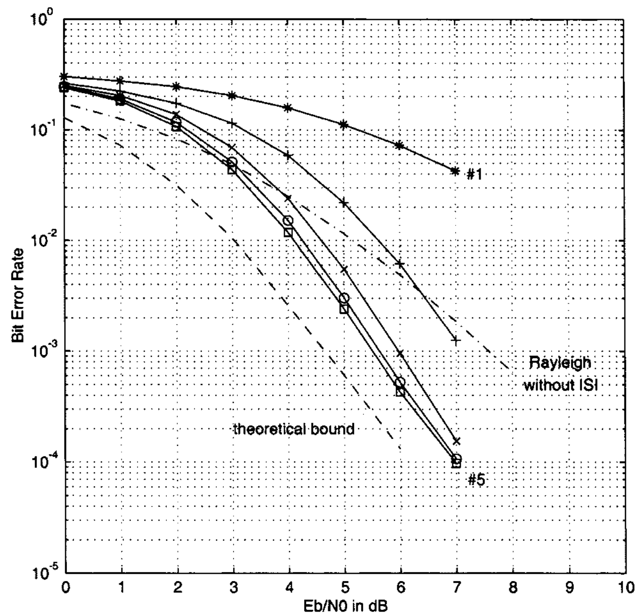

Fig. 11. Turbo-equalization performance over a multipath Rayleigh channel for a 4-QAM modulation.

turbo-equalizer performance is suboptimum because the equalizer outputs are correlated and there is a loss of the channel decoding gain. Simulations show that the interleaver must very large when the channel is highly selective.

B. Time-Varying Channels

Radio communication propagation is generally subject to multipaths corrupted by Doppler effects, which depend on the relative speed between the emitter–receiver and the carrier frequency. The channel coefficents may be modeled by a complex-valued independent process which may be expressed as

$$h_l(n) = \sqrt{\frac{P_l}{N}} \sum_{i=1}^{N} e^{j(2\pi(f_d \cos \xi_{l,\,i})nT + \psi_{l,\,i})} \qquad l = 0, \ldots, L$$

where f_d and P_l correspond to the maximum Doppler and at the mean power associated with the l path, respectively. Parameters $\xi_{l,\,i}$ and $\psi_{l,\,i}$ are uniform random variables over $[0;\ 2\pi]$. For simulations N was fixed to 10. Generally the Doppler effect is characterized by the product of a Doppler band $B_d = 2f_d$ by T.

For simulations, the information data were coded by a 1/2 rate convolutional code with generator polynomials equal to 23, 35. The turbo-equalizer performance was evaluated for 4-QAM signalling schemes over a Rayleigh channel. The B_dT parameter is fixed to 0.001.

Data with variance $\sigma_d^2 = 1$ are assumed to be emitted by slots of 125 symbols whose first 25 symbols are known, from the receiver. Thus, the training sequence represents 20% of the transmission flow. All the slots are sequentially transmitted over the continually varying Rayleigh multipath channel. The loss of 1 dB in the ratio E_b/N_0 due to the use of a periodic training sequence was not taken into account for the plotted curves.

The algorithm used with the Rayleigh channel is described in Section III-B. The transversal equalizer $(p = 1)$ has nine coefficients. This value is weak and can involve some performances loss. Nevertheless, it necessary to have a weak number of coefficients in order to enable the RLS algorithm to follow the time-varying channel. The central coefficient is initialized to one and the weighting factor equal to 0.965. For the other iterations $(p > 1)$, the equalizer coefficients are calculated from the estimated coefficients channels, which were previously obtained from an RLS algorithm. The number of taps for the channel estimator is equal to 5 and the weighting factor 0.965. The BER was evaluated for at least 500 errors at the last iteration.

Results presented in Fig. 11 are given for a Rayleigh channel which has three paths with the same power mean and each path is separated by a symbol duration T. A 128×128 matrix following a nonuniform law performed the interleaving.

We have represented by a dashed line the theoretical bound of the turbo-equalizer, which corresponds to an optimum IC fed by transmitted symbols. The turbo-equalization goal is to reach the theoretical bound. At the optimum IC output, ISI is completely cancelled and the energy from the different channel taps is collected. This explains the diversity gain in comparison with the Rayleigh non frequency selective channel plotted by a dashed–dotted line. After five iterations, performance of the turbo-equalizer is close to the theoretical bound, which indicates a good behavior of this new receiver for a large class of channels.

V. Conclusion

This paper describes a reduced complexity receiver for a M-QAM, called a turbo-equalizer, that uses equalization and coding jointly optimized in an iterative process. For a large class of frequency-selective channels, turbo-equalization allows ISI to be totally overcome and reaches the coded Gaussian channel performance that actually seems to be a theoretical bound. Moreover, using an adaptive equalizer allows high-order modulation over channels with a large delay spread to be processed, which is impossible with a conventional Viterbi detector (MLSE). To achieve the turbo-equalizer, a SISO M-ary channel decoder has been used, the complexity of which is practically independent of the modulation order. Finally, simulations over a radiomobile-type channel show that turbo-equalization could be used for all digital receivers when information data are coded and interleaved.

REFERENCES

[1] C. Laot, "Egalisation autodidacte et turbo-ègalisation. Application aux canaux sélectifs en fréquence," Thése de l'Université de Rennes 1, Juillet, 1997.

[2] A. Glavieux, C. Laot, and J. Labat, "Turbo-equalization over a frequency selective channel," in *Symp. on Turbo-Codes*, Brest, France, Sept. 1997.

[3] C. Laot, A. Glavieux, and J. Labat, "Turbo-égalisation," Brevet France Télécom, May, no. 9 705 978, 1997.

[4] A. Gersho and T. L. Lim, "Adaptive cancellation of intersymbol interference for data transmission," *Bell Syst. Tech. J.*, vol. 60, no. 11, pp. 1997–2021, Nov. 1981.

[5] M. S. Muller and J. Salz, "A unified theory of data-aided equalization," *Bell Syst. Tech. J.*, vol. 60, no. 9, pp. 2023–2038, Nov. 1981.

[6] M. Vedat Eyuboglu, "Detection of coded modulation signals on linear, severely distorted channels using decision feedback noise prediction with interleaving," *IEEE Trans. Commun.*, vol. 36, pp. 401–409, Apr. 1988.

[7] K. Zhou and J. G. Proakis, "Decision feedback equalization of time-dispersive channels with coded modulation," *IEEE Trans. Commun.*, vol. 38, pp. 18–24, Jan. 1990.

[8] P. Didier, "La turbo-égalisation et son application aux communications radiomobiles," Thése, présentée ǎ l'UBO, Apr. 26, 1994.

[9] C. Douillard, A. Picart, P. Didier, M. Jézéquel, C. Berrou, and A. Glavieux, "Iterative correction of intersymbol interference: Turbo-equalization," *Eur. Trans. Telecommunications*, vol. 6, no. 5, Sept./Oct. 1995.

[10] C. Berrou and A. Glavieux, "Near optimum error correcting coding and decoding: Turbo-codes," *IEEE Trans. Commun.*, vol. 44, pp. 1262–1271, Oct. 1996.

[11] J. G. Proakis, *Digital Communications*. New York: McGraw-Hill, 1989.

[12] S. U. H. Quershi, "Adaptative equalization," *Proc. IEEE*, vol. 73, pp. 1349–1387, Sept. 1985.

[13] D. D. Falconer, "Jointly adaptive equalization and carrier recovery in two dimensional data communications systems," *Bell Syst. Tech. J.*, vol. 55, pp. 317–334, March 1976.

[14] P. Vila *et al.*, "Reduced-complexity M-ary binary decoders for turbo-equalization," in *2nd Int. Symp. Turbo Codes and Related Topics*, Brest, France, Sept. 4–7, 2000.

[15] A. J. Viterbi, "An intuitive justification and a simplified implementation of the MAP decoder for convolutional codes," *IEEE J. Select. Areas Commun.*, vol. 16, pp. 260–264, Feb. 1998.

[16] C. Berrou, P. Adde, E. Angui, and S. Faudeil, "A low complexity soft-output Viterbi decoder architecture," in *ICC'93*, Geneva, Switzerland, May 1993.

[17] B. Porat and B. Friedlander, "Blind equalization of digital communications channels using high-order moments," *IEEE Trans. Signal Processing*, vol. 39, pp. 52–526, Feb. 1991.

Christophe Laot was born in Brest, France, on March 12, 1967. He received the Eng. degree from the Ecole Francaise d'Electronique et d'Informatique (EFREI), Paris, France, in 1991 and the Ph.D. degree from the University of Rennes, Rennes, France, in 1997.

He is currently Associate Professor with the Digital Communications Team, Ecole Nationale Supérieure des Télécommunications de Bretagne (ENST Bretagne), Brest, France. His professional interests include intersymbol interference, equalization, channel coding, turbo-equalization, and interference suppression in CDMA systems.

Alain Glavieux was born in France in 1949. He received the Eng. degree from the Ecole Nationale Supérieure des Télécommunications, Paris, France in 1978.

He joined the Ecole Nationale Supérieure des Télécommunications de Bretagne, Brest, France, in 1979, where he is currently Director of Corporate Relations. His research interests include channel coding, communications over fading channels, and digital modulations.

Joël Labat was born in Dakar, Sénégal, in 1951. He received the Eng. degree from the Conservatoire National des Arts et Métiers (CNAM), Brest, France, in 1989, and the Ph.D. degree from the University of Bretagne Occidentale (UBO), Brest, France, in 1994.

He is presently with the Ecole Nationale Supérieure des Télécommunications de Bretagne (ENST Bretagne), Brest, France, as Professor. His research interests include digital communications over multipath channels and related problems such as blind equalization, synchronization, and signal processing. His favorite fields of investigations are both underwater acoustic communications and wireless communications.